Doktor et al. *Journal of Mathematics in Industry* (2018) 8:10
https://doi.org/10.1186/s13362-018-0052-5

Journal of Mathematics in Industry
a SpringerOpen Journal

RESEARCH

Open Access

Characterization of steel buildings by means of non-destructive testing methods

Markus Sebastian Doktor[1,2*], Christian Fox[2], Wolfgang Kurz[2] and Jean-Pierre Stockis[1]

*Correspondence:
doktor@mathematik.uni-kl.de
[1] Mathematics Department, Technische Universität Kaiserslautern, Kaiserslautern, Germany
[2] Department of Civil Engineering, Technische Universität Kaiserslautern, Kaiserslautern, Germany

Abstract

Non-destructive testing methods became popular within the last few years. For steel beams incorporated in buildings there are currently only destructive ways for testing the yield limit as well as for determination of the current stress level. Rise of ultrasonic and micro-magnetic tools for (non-destructive) measurements allows the characterization of the inbuilt material especially of old steel bridges as economical maintenance of the infrastructure. It is possible to determine the reserve of residuence of bridges or of any other existing steel buildings in order to upgrade them competitively for future usage by the possibility of a simple way of strengthening by welding or using bolds. This is done using modern devices for ultrasonic and micro magnetic data recording on the one hand and modern techniques from nonparametric statistics such as sieve, partition and semi-recursive estimators on the other hand.

Keywords: Nonparametric regression; Robust regression; Mathematical and mechanical modeling; Dependency modeling; Civil engineering; Non-destructive testing; Material characterization

1 Introduction

The load bearing capacity in existing buildings is classically determined by means of load tests. If a calculation model gives no sufficient results, highly complex test loadings have to be done to determine the load bearing capacity. For verification in existing buildings material characteristics as the yield strength and the existing stresses have to be known, determining them non-destructively is an obvious advantage. Furthermore, the internal forces could be estimated, which includes second order theory as well as e.g. imperfections and signal denoising (outlier detection). This is crucial for the verification of (sufficient) load bearing capacity. The appointed lifetime of a new building is 50 to 100 years. Especially for steel buildings, with high variations but well known material characteristics, extensions of the lifetime in the sense of sustainability might be possible, cf. [1]. The actual standards for condition monitoring are in [2, 3] with [4, 5] explaining how to localise fatigue effects before crack initiation starts. Therewith mechanical stresses can be obtained via electromagnetic induced ultrasonic measurements and acusto-elastic effects, cf. [6, 7]. Thus, mathematical modeling is necessary for the micromagnetic records to determine material characteristics, the ultrasonic records to determine the current state of load and finally generalising the mechanical model to estimate the internal forces. This work links the non-destructive records with modeling and the generally accepted engineering standards.

2 Non-destructive testing methods

To determine the residual carrying capacity of a construction without risk of collapse is just possible with non-destructive testing methods. The determination of the yield strength by micromagnetic measurements and the determination of the current load state by ultrasonic measurements are described below.

2.1 Unknown material characteristics

The yield strength is the most important material characteristic of the steel to determine the load-bearing capacity. It is defined via regulations to characterize different steel qualities. If the yield limit is determined by measurements, the ultimate limit state design can be proven by real material characteristics without model uncertainties and not by guaranteed minimum values. For determination of the yield strength of an investigated beam the ferromagnetic properties of steel are used. There is a causal relation between magnetism and the yield limit to be determined, see [8] for details. For calibration means, the magnetic properties of the different steel types are determined and assigned to their yield limit measured in a classical tensile test.

2.2 Determination of the current load state

The determination of the current state of stress of a built-in steel beam is possible via ultrasonic measurements, compare [7, 9, 10]. The influence of the stress and strain conditions on the speed of the propagation of the ultrasonic waves is used for the ultrasonic stress analysis. Comparing the speed of the ultrasonic waves in a beam without load v_0 and the speed in a beam with load v_l, the current state of stress ς (in $\frac{\mathrm{N}}{\mathrm{mm}^2}$) can be determined using the following equation:

$$\varsigma = \frac{(v_0 - v_l)}{v_0} \cdot \frac{K}{H}, \tag{1}$$

$\frac{K}{H}$ is a linear factor, a so-called acusto-elastic constant, that is determined in lab tests, compare Fig. 1. In these tests the speed v_0 is measured in beams without load. In practice, there is no possibility for a direct measurement as there are no in-built beams without load. Due to the anti-symmetric stress distribution in the cross section of a beam, the speed v_0 can be determined by the mean value of symmetrically distributed measurement

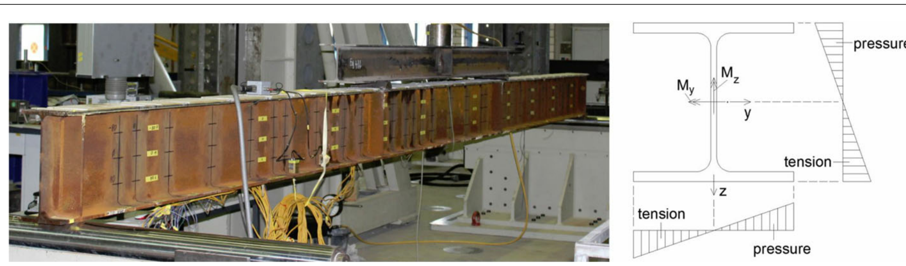

Figure 1 *Left:* Beam in lab test. *Right:* Anti-symmetric stress distribution in the cross section

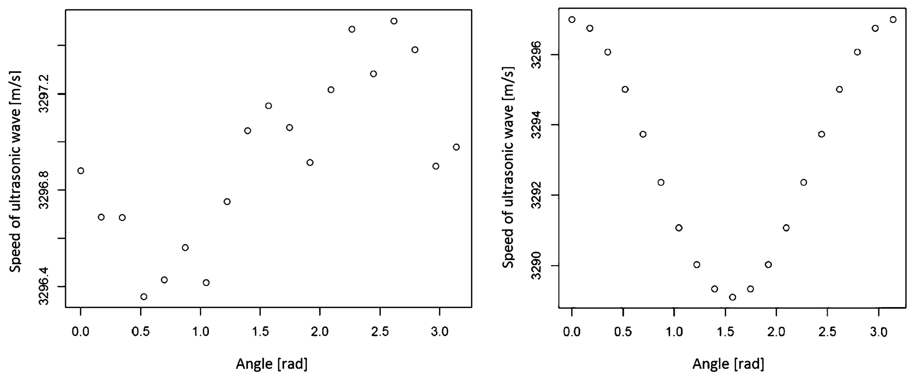

Figure 2 *Left:* Speed variation influenced by stress. *Right:* Speed variation due to texture

points in a loaded beam assuming that there is no axial force. The texture due to the rolling process of a steel beam causes the directional property of the ultrasonic measuring results (anisotropism). The difference of the speed according to the texture is shown in Fig. 2, *Right* and the difference of the speed according to the stress due to loading is shown in Fig. 2, *Left*. Ultrasonic measurement values are the addition of both of them. The influence of texture is up to ten times higher than the influence of stresses. To show a sufficient bearing resistance, the much greater influence of texture has to be eliminated.

3 Construction & measurements in existing buildings

3.1 Construction

Higher static loads can easily be supported by steel constructions with simple strengthening measures. But the used steel and its material characteristics, especially his bearing capacity, are not known. Furthermore, the current state of load is typically unknown. Modifications of buildings in their previous service lifes caused changed load transfers, which are not incorporated in current construction plans. In many cases, construction plans of the building to be investigated do not exist anymore. Thus, it is impossible to make a serious statement about the load bearing capacity still available in the beams.

3.2 Recording data

Recording data in an existing building is a grueling task which has to be improved. The measurement equipment needs external electrical power supply and should be adapted to run with a battery to make it more handy, unless the devices themselves are quite small and handy, compare Fig. 3 and Fig. 4. Nevertheless, measurements have been made at the materials testing institute (MPA) of the University of Kaiserslautern as well as in existing buildings like the Ceasarparkbrücke (Kaiserslautern), see Fig. 5, and a covered market (Frankfurt/Main), see Fig. 4. In the sequel, the data evaluated in Sect. 5 are those obtained in the lab test because the exact load situation is known, thus, we have structural as well as measured residuals for the evaluation of the techniques.

4 Mathematical modeling and applications

The necessity of fitting a regression model instead of solving a linear equation system is quickly explained: we have in-data-dependencies which are modeled as stochastic dependencies on the one hand, furthermore linear dependencies due to the statical system

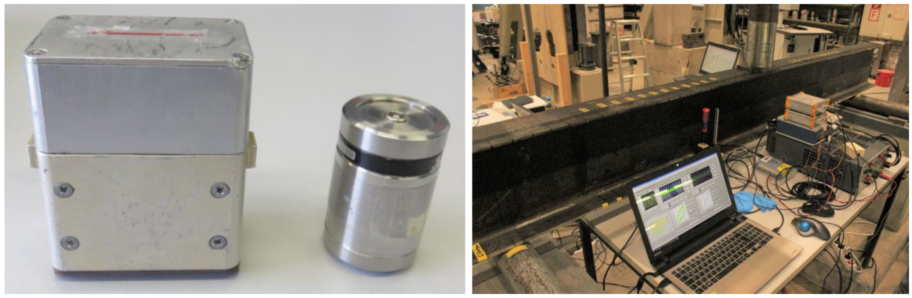

Figure 3 *Left:* Both sensors for recording ultrasonic runtimes and micromagnetic. *Right:* A coated steel beam in the lab with devices to record ultrasonic signals as well as micromagnetic quantities. The notebook in front shows hysteresis curves surveilling the micromagnetic records used for the determination of the yield strength

Figure 4 *Left:* An AScan which gives, via peak-to-peak-analysis, the time-of-flight of the ultrasonic waves to estimate the stress. *Right:* Recording data in the market hall

Figure 5 *Left:* The Caesarparkbrücke in Kaiserslautern. *Right:* Optimal Measurement Conditions on coated beam

(compare Fig. 6 for a complex statical example) which makes an application of the Gaussian algorithm (or something equivalent) insufficient on the other hand. To fit a regression model to the data, we need to develop a stochastic model of the ultrasonic measurements. The time-of-flight of the ultrasonic wave in every point measured should be related to the local stress in the beam. Additionally, the residuals have to be taken into account for (stochastic) dependency modeling. Finally, a segmented regression approach based on the statical system and statistical decision criteria, was developed, for details see [9, 11] as a prequel to the estimation of the internal forces, with algorithms implemented in MATLAB and R, cf. [12, 13]. Unless the times-of-flight are observed in practice we work with simulated stresses according to equation (1) in the sequel to simplify notation.

Figure 6 *Left:* The 7 traces times-of-flight are recorded in as a cross section (compare Abb. 5.25 in [9]). *Right:* An overview about the amount of beams and, thus, complexity of records and changes of the statical system

4.1 Mathematical and mechanical models

The stresses existing in a steal beam can be decomposed in different sources of stress via classical/technical mechanics, see e.g. [9]. For security and safety concepts, we have to decompose them in their single parts: normal (N) and residual (E) stress, stress due to bending around the y or z axis (M_y and M_z, respectively) and stress due to warping torsion (M_w). The concept of measuring points uses symmetry as far as possible and looks, locally in every cross section of the steel beam along the x-axis, as follows:

This leads to the following identities for the local stresses which has to be handled mathematically, compare Fig. 6 and [14] for details:

$$\varsigma_1(x) = \frac{z_1}{i_y} M_y(x) + \frac{y_1}{i_z} M_z(x) + \frac{q_1}{i_w} M_w(\varepsilon x) + E_1 + N, \tag{2}$$

$$\varsigma_2(x) = \frac{z_2}{i_y} M_y(x) + \frac{y_2}{i_z} M_z(x) + \frac{q_2}{i_w} M_w(\varepsilon x) + E_2 + N, \tag{3}$$

$$\varsigma_3(x) = \frac{z_3}{i_y} M_y(x) + E_3 + N, \tag{4}$$

$$\varsigma_4(x) = E_4 + N, \tag{5}$$

$$\varsigma_5(x) = \frac{z_5}{i_y} M_y(x) + E_5 + N, \tag{6}$$

$$\varsigma_6(x) = \frac{z_6}{i_y} M_y(x) + \frac{y_6}{i_z} M_z(x) + \frac{q_6}{i_w} M_w(\varepsilon x) + E_6 + N, \tag{7}$$

$$\varsigma_7(x) = \frac{z_7}{i_y} M_y(x) + \frac{y_7}{i_z} M_z(x) + \frac{q_7}{i_w} M_w(\varepsilon x) + E_7 + N \tag{8}$$

with known constants from geometry: ε, i_y, i_z, i_w, z_j, y_j, q_j, $j = 1, \ldots, 7$. We will use $g_i = (g_{y_i}, g_{z_i}, g_{w_i}) = (\frac{z_i}{i_y}, \frac{y_i}{i_z}, \frac{q_i}{i_w})$ in Sect. 4.3 to shorten notation. Assume the bending moments M_y, M_z to be polynomials of degree at most $n \in \mathbb{N}$ and the warping torsion to be some hyperbolic function, i.e. $M_w(x) = a + b\sinh(\varepsilon x) + c\cosh(\varepsilon x) = a + b\sinh_\varepsilon(x) + c\cosh_\varepsilon(x)$, $a, b, c \in \mathbb{R}$ (see e.g. [9] for details). Note, that all the mechanical moments could be trivial in reality, which is also covered in the mathematical model. A sketch of the procedure of computing the mechanical moments will be given in Sect. 4.3 after dependency modeling in Sect. 4.2.3 and (nonparametric) outlier detection in Sect. 4.2.2.

4.2 Regression model for segmented stress estimation and dependency modeling

Due to the statical system we expect the stress curve to show interval-wise different behaviour. The points of change of the (local) regression function, driven by the stress curve, are well known through the statical system.

4.2.1 The regression model

For observations points $x_1, \ldots, x_N$, we want to estimate the measured stresses $\varsigma_1, \ldots, \varsigma_N$, i.e. for all $1 \leq j \leq N : \varsigma_j = f(x_j) + \epsilon_j$, where ϵ_j is the residual term, compare equation (1). This stresses are driven by a polynomial and a hyperbolic term. The classical minimization problem in linear regression for a third order polynomial and hyperbolic terms looks as follows:

$$\min_{a,b,c,d,e,f} \sum_{k=1}^{N} \left(\varsigma_k - a - bx_k - cx_k^2 - dx_k^3 - e \sinh_\varepsilon(x) - f \cosh_\varepsilon(x)\right)^2.$$

Due to practical reasons, we restrict ourselves to (piecewise) degree three polynomials with hyperbolic terms and a fixed natural number K of segments, the permitted number of different regression functions. The equation to be minimized, where the I_js are in increasing order with $\bigcup_j I_j = \{x_1, \ldots, x_k\}$, is

$$\min_{L=1,\ldots,K} \sum_{j=1}^{L} \min_{\substack{a_j,b_j,c_j,\\ d_j,e_j,f_j}} \sum_{k \in I_j} \left(\varsigma_k - a_j - b_j x_k - c_j x_k^2 - d_j x_k^3 - e_j \sinh_\varepsilon(x) - f_j \cosh_\varepsilon(x)\right)^2.$$

Further, a_j, b_j, c_j, d_j, e_j, f_j are the coefficients of the jth regression function, i.e. the ones for the interval I_j. Additional knowledge of the statical system reduces the computational effort: only in load introduction points of the system a change of the function is permitted. This is an additional criterion in the minimization as well as the R^2-statistic to be minimized and based on [11]. Furthermore outliers are a serious problem in practice and the residuals show a dependency structure (in particular, they seem neither independent nor normally distributed in contrast to the Gauss-Markov Theorem, see Sect. 4.2.3). Our approaches to this tasks are presented in detail in the following subsections.

4.2.2 Statistical tests for outlier detection

The devices used for data-recording are error-prone. This means that a lot of work has to be done to eliminate/minimize the systematic error occurring due to the measuring devices, compare Fig. 7. At a first glance physically non-plausible records were eliminated using a fixed-deviation criterion based on the literature, compare [9]. This reduces on the one hand the amount of errors recorded, on the other hand the number of records available. A statistical test based on the median and asymptotics of order statistics has been developed to solve this problem, for details on multiple testing see [15]. It works as follows: for a dataset $z = (z_1, \ldots, z_N)$ compute the median $\tilde{z}$, the 25% and 75%-quantiles and their distance $\tilde{z}_{25}$, $\tilde{z}_{75}$ and $\tilde{z}_{\text{diff}}$, respectively. Those recorded values satisfying $|z_i - \tilde{z}| > b \cdot \tilde{z}_{\text{diff}}$

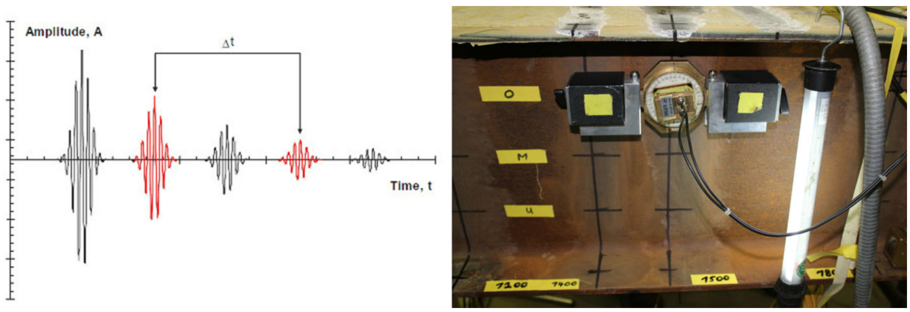

Figure 7 *Left:* One source of errors is missing one of the echos (compare Abb. 3.7 in [9]). *Right:* Precise preparation is necessary for feasible measurements

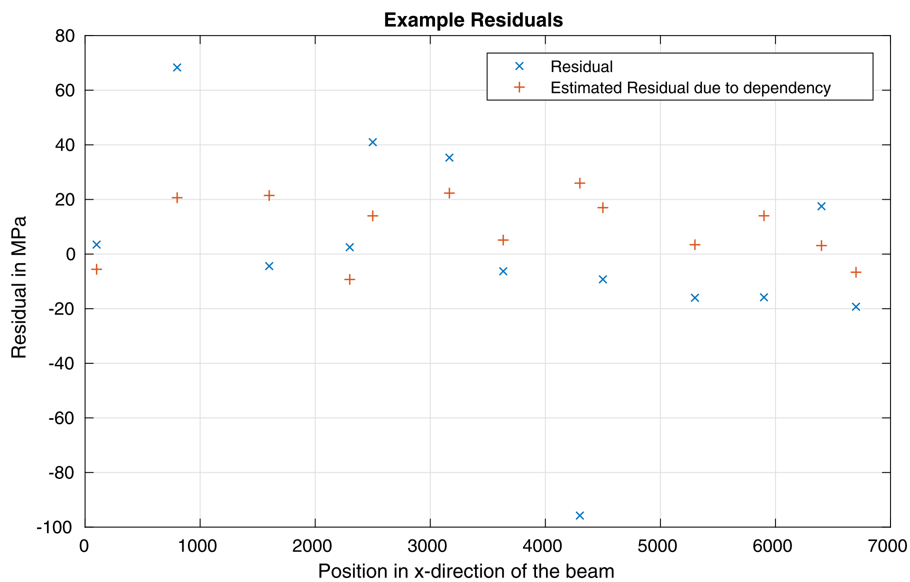

Figure 8 Residuals from real data analysis in one trace, hence 1- and not 7-dimensional. On the one hand with non-zero mean, on the other hand with structure (here: heteroskedastic, predictable). Note, that this is just a small example neither indicating nor including all information available

where $b > 0$ is the bandwidth (chosen according to the robustly estimated standard deviation and the asymptotics of order statistics to get the desired α-level, see [16] are classified as outliers. This significantly improves the results unless robust methods according to [17] have been used, e.g. a Mahalanobis-distance based outlier test. This has been highlighted to be unsatisfactory for practical problems, e.g. due to numerical inconsistencies. They occurred in the computation of the regression curve with confidence bands of range $1100\,\frac{\mathrm{N}}{\mathrm{mm}^2}$. This is rather far away from the prevalent yield limit of $235\,\frac{\mathrm{N}}{\mathrm{mm}^2}$ in typical steel beams incorporated. Thus, additional effort has to be done for dependency reduction.

4.2.3 Dependency modeling

For a real data example, the residuals $\epsilon_j = \varsigma_j - f(x_j)$ from a small dataset can be seen in Fig. 8: Dependency measures such as Copulas indicate dependency too. Possible physical reasons are, beneath others, the induced magnetic field while measuring with electromagnetically induced ultrasonc waves or the local orientation of the germ-grain structure of steel, compare [4, 5, 18]. Therefore, a model for the dependencies has to be developed, in this case a non-causal time series approach which could model material and device influences from neighbouring points of measurement. This makes it impossible to use classical estimates, e.g. Yule-Walker-Estimates, for this problem, see [19] for details. The solution to dependency modeling ends up to be a non-causal Moving Average process of order 4, i.e. we model the residual ϵ_k from the segmented regression model via

$$\epsilon_k = \sum_{j=-2,-1,1,2} \alpha_j \cdot \epsilon_{k+j} + \delta_k$$

for finite and bounded $\alpha_j, j = -2, -1, 1, 2$ and new independent zero-mean residual δ_k. The estimation of parameters has to be done via computationally expansive combined bisection and grid-search, unless other techniques for estimation in non-causal settings are available. Nevertheless, this gives opportunity to:

(i) Continue with the model with corrected dependency structure

(ii) Restart the estimation procedure with reduced influence due to dependency.

The procedure of choice is the second in order to stay with classical security/safety concepts and apply methods from nonparametric statistics. Thus, for simulated data (the coefficients of time series are theoretically zero) as well as for real data (where we expect such dependencies) we start with the regression model according to Sect. 4.2.1 and do the dependency treatment presented here to continue with the estimation of the internal forces in Sect. 4.3. Furthermore, this states that the unique estimation of the internal forces using a linear equation system is in general not possible.

4.3 Local regression estimates for internal forces

Using the symmetries shown in equations (2) to (8) and known constants from geometry the estimation is based on partitioning and sieving the observations in the different traces, compare Fig. 9 to 11. This is done in (up to) six steps, for description purposes with data generated via finite-element simulation in the description and real data subsequently, with least squares for each local estimation, starting with an initial value $\theta^0 = (\alpha_0^0, \dots, \alpha_{n_1}^0, \beta_0^0, \dots, \beta_{n_2}^0, \gamma_0^0, \gamma_1^0, \gamma_2^0)$ from mechanics for the internal forces M_y, M_z, M_w, respectively, the exponent is an index for the estimation step, the coefficients $n_1, n_2 \geq 0$ are the polynomials degrees. Furthermore, we use $\tilde{\alpha}$, $\tilde{\beta}$, $\tilde{\gamma}$ to denote the moments' constants multiplied with the geometry factors to obtain stresses. The procedure works as follows:

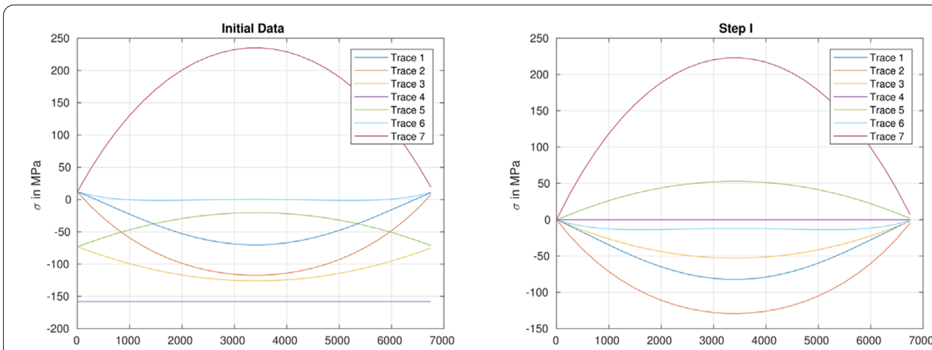

Figure 9 *Left:* Example input for a fork-mounted single-carrier. *Right:* After normalisation

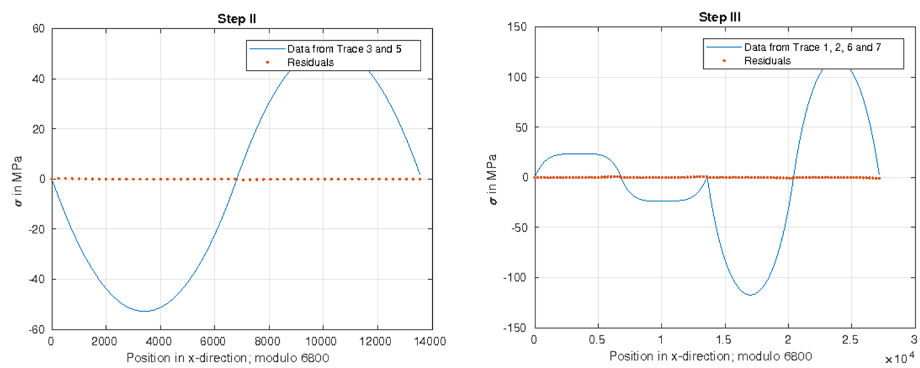

Figure 10 *Left:* Estimation of M_y. *Right:* Estimation of $M_z + M_w$

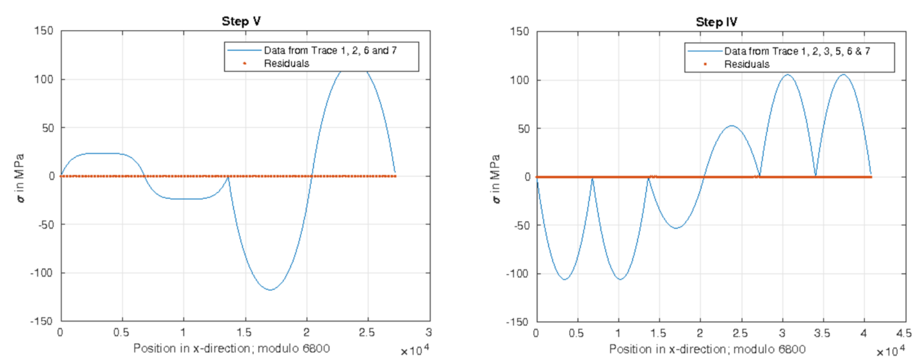

Figure 11 *Left:* Update of the estimation of M_y. *Right:* Update of the estimation of $M_z + M_w$ and termination

Algorithm First, normalise all observations, i.e. remove the constants $c = (c_1, \dots, c_7)$, and keep them for estimation of the occurring constants α_0, β_0, γ_0. The part left is the sum of normal and residual stress. Note, that the separation in residual and normal stress (i.e. splitting the constant) is not possible in general unless further information, e.g. from micro magnetics, see Sect. 4.5, are available.

Second, estimate the internal force M_y from traces 3 and 5 using (robust) Least Squares (cf. [20]) under the constraint $|\tilde{\alpha}_0^1| \leq |c_3|, |c_5|$. The estimate obtained is called $\theta^2 = (\alpha_0^2, \dots, \alpha_{n_1}^2, \beta_0^0, \dots, \beta_{n_2}^0, \gamma_0^0, \gamma_1^0, \gamma_2^0)$ (analogously without mentioning in the sequel).

Third, estimate the internal forces $M_z + M_w$ (note, that they are either both trivial/constant or linearly independent, thus, there is a unique solution to this estimation problem) in traces $1, 2, 3, 5, 6, 7$ under knowledge of M_y (i.e. subtraction) from the previous step and keep the constraints $|\tilde{\beta}_0^3 + \tilde{\gamma}_0^3 + \tilde{\alpha}_0^2| \leq |c_1|, |c_2|, |c_6|, |c_7|$.

Fourth, as first update step, estimate the internal force M_y using the information in all traces (except trace 4) under knowledge of M_z and M_w (i.e. subtraction) from the previous step (see Fig. 10) and keep the constraints $|\tilde{\beta}_0^3 + \tilde{\gamma}_0^3 + \tilde{\alpha}_0^4| \leq |c_1|, |c_2|, |c_6|, |c_7|$.

Fifth, as second update step, estimate the internal forces $M_z + M_w$ in traces $1, 2, 6, 7$ under knowledge of M_y from the previous step (see Fig. 11) and keep the constraints $|\tilde{\beta}_0^5 + \tilde{\gamma}_0^5 + \tilde{\alpha}_0^4| \leq |c_1|, |c_2|, |c_6|, |c_7|$.

Sixth, check whether $\|\theta^4 - \theta^5\| < \kappa$ for a previously fixed constant $\kappa > 0$ (i.e. a Cauchy sequence criterion) or repeat updating the estimates under all information available in

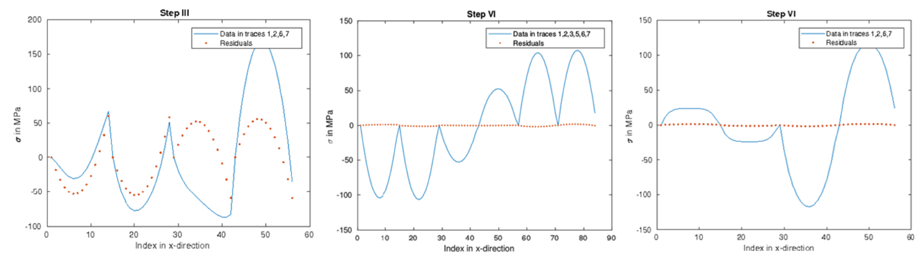

Figure 12 Example of a contaminated dataset with less points and reasonable result after 36 iterations

random and non-repeating order at most M times, checking the Cauchy criterion after each iteration.

An example with less and contaminated data and bad initial values, including the necessity of the last step, can be seen in the following Fig. 12: The trend in the residuals is quite clear: starting point is a quite bad initial value which gets better and better with an increasing number of iterations. This corresponds to two effects in the construction of the estimates: First, we use the least squares approach by Howard and Welsh (compare [20]), which avoids deterioration of the estimate. Second, the ping-pong between different datasets improves the local estimates, thus, the global ones. Therefore, we can clip the following:

- Weaker dependence structures are crucial for the application of the estimation techniques, therefore, the dependency reduction was necessary.
- The constants α_0, β_0, γ_0 can not be estimated simultaneously in steps 3 and 5, thus, a fixed-constant approach has to be chosen including several trials.
- A deterioration of the local estimation is not possible due the construction of the Levenberg-Marquardt least squares, cf. [21, 22].
- Using the geometry constants from equations (2) to (8) and the estimates α_0, β_0, γ_0 from the final estimation, the remaining parts of c, $\tilde{c}$ is the estimate for the sum of residual and normal stress and with knowledge of the normal stress, a decomposition in residual and normal stress can be done, see [18].
- An absolute value bound (or in some cases: estimate) for the normal stress could be obtained via

  $$N = \min_{i=1,\dots,7} \left\{ \left| c_i - (g_{y_i} \cdot \alpha_0 + g_{z_i} \cdot \beta_0 + g_{w_i} \cdot \gamma_0) \right| \right\},$$

  an estimate for the residual stresses is given via

  $$E_i = c_i \pm N - (g_{y_i} \cdot \alpha_0 + g_{z_i} \cdot \beta_0 + g_{w_i} \cdot \gamma_0).$$

  Note, that those estimates are not necessarily consistent ones.
- If there is no feasible solution to the estimation problem, plasticising areas might have been identified/detected. A local decrease of residual stress (*internal forces devour residual stress*, cf. [18]), i.e. searching in double of the yield limit (see Sect. 4.5) for the constants is the approach of choice in this case.

4.4 Properties of the estimates

The estimates in this procedure are partition, sieve and semirecursive estimates, unless the procedure to estimate within this steps locally is a (robust) version of the Levenberg-Marquardt Algorithm, compare [17, 20–23].

Theorem 1 (Doktor, Stockis) *Let M_y, M_z be polynomials of degree at most $n \in \mathbb{N}$. Further, let M_w be a hyperbolic function (i. e. the mechanical model is stated properly). Furthermore, let the tuple $(x_i, \varsigma_i)_{i=1,\dots,N} \in \mathbb{R}^8$ be pairwise uncorrelated with finite expectation $|\mu| < \infty$ and uniformly bounded variance $0 < \sigma^2 < \infty$.*

Then the estimates used in every step are consistent. Furthermore, θ is a consistent estimate for the coefficients of the internal forces.

Proof The statement follows mainly from the Theorems 10.3, 20.3 and 24.1 in [23] and Slutsky's Lemma. □

Theorem 2 (Doktor, Stockis) *Consider the setup of Theorem 1. Then the estimates obtained for the internal forces are asymptotically normally distributed.*

Proof The statement for sieve and partition estimates follows from consistency and Theorems 11.4 and 21.1 in [23], the final statement uses additionally the rules of calculus for the multivariate normal distribution. □

Note, that this statement can be generalized in a robust setting according to [17] unless the rate of convergence decreases which is of high importance in practical applications as recording data is time-consuming and might be expansive.

4.5 Further improvement with micromagnetics

The determination of valid confidence bands is a necessity for proper safety concepts in civil engineering. Further, the classification of residuals observed in ultrasonics has to be done properly to avoid economical and ecological disadvantages. Based on [18], additional micromagnetic measurements are used to link techniques and concepts.

4.5.1 Reduction of complexity

The devices used to record micromagnetic quantities measure 42 different quantities. They use four different implemented sensors which are rather expensive. To make the device handable in practice, a goal is the reduction of the number of quantities necessary without significant loss of quality. For this purpose we applied multiple statistical tests of independence, based on χ^2-tests, for details, we refer to [15]. With a (combined) level of 10%, 36 quantities are identified to be stochastically dependent. The quantities left are driven by two sensors only: the Barkhausen effect and incremental permeability, which halves the amount of sensors required, see [8] for details.

4.5.2 Combining ultrasonic waves and micromagnetism

The link function is based on stochastic moments of the kernel density estimate of the micromagnetic measurements. In practice, several thousand micromagnetic observations are available for every single trace $j = 1, \dots, 7$ of the cross section in x, making a proper

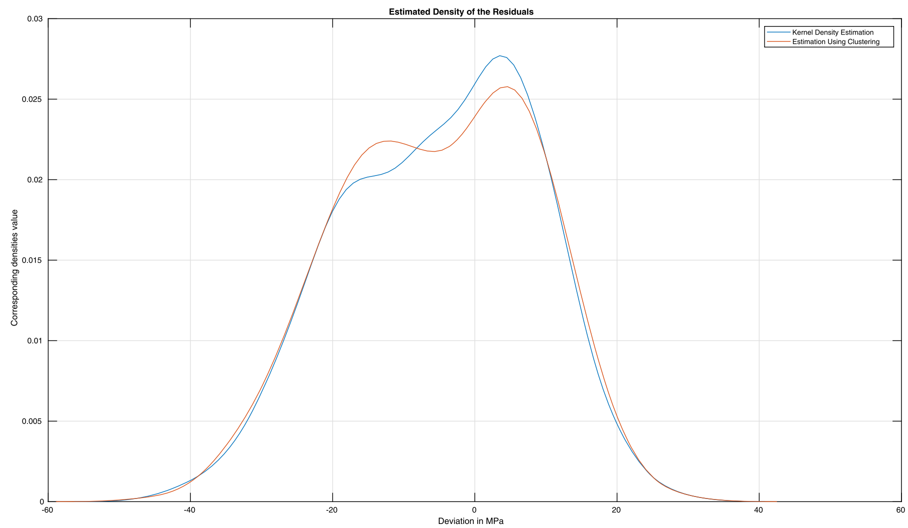

Figure 13 The density of the distribution of the residuals estimated using a Gaussian kernel and measurements is given in blue, the mixture of the densities estimated using the link-function in orange. The difference is minimal due to bias-effects which vanishes asymptotically

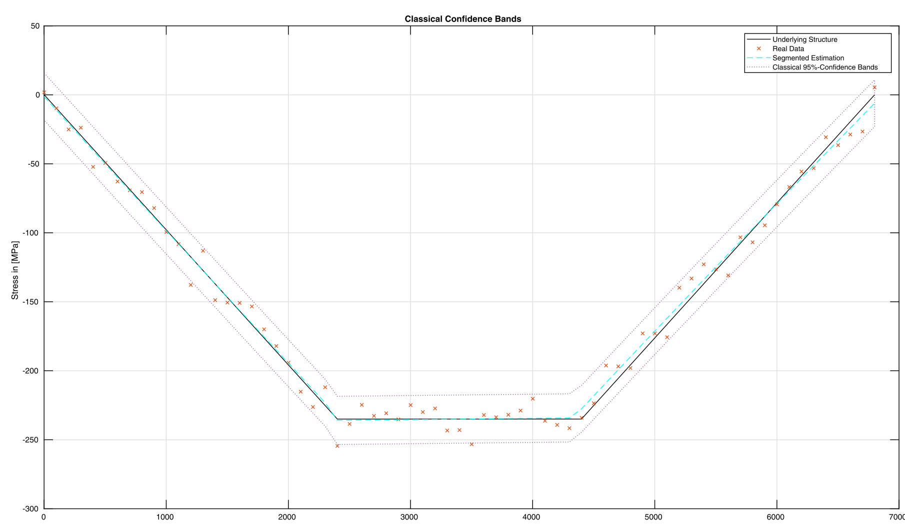

Figure 14 The analytic (blue) curve, the under idealised conditions recorded data (orange) the estimated curve (cyan) with confidence bands (purple)

estimation of the stochastic moments possible. It allows the adaption of the confidence band given the distribution of the residuals specifically for all points. Assuming the link-function to be consistent, the parameter of the mixture of Gaussians could be estimated consistently, see Fig. 13 and cf. [24], for details, with known asymptotic distribution and the following confidence bands for a 4-point-bending-test, see Fig. 14 and Fig. 15. Finally, the combination of the yield limit gives bounds for the constants $\tilde{c}$ and might lead to the decomposition of the constant in residual and normal stress or the identification of plasticising areas, see [18] for details.

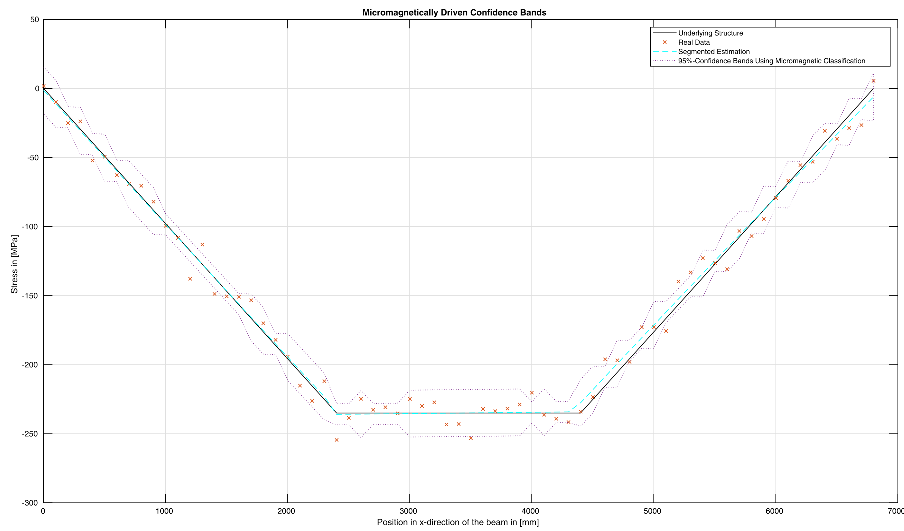

Figure 15 The analytic (blue) curve, the under idealised conditions recorded data (orange) the estimated curve (cyan) with smaller confidence bands (purple) compared to the classical setup

5 Discussion and results

5.1 A simulation example

The estimation technique described in Algorithm has been applied to datasets generated via Finite-Element simulation. The example inputs were an IPE 360, length 6800 mm and fork-mounted single-carrier with line load only which reduces the amount of variables to be estimated. The internal forces for the simulation are analytically given as

$$\begin{aligned}
M_y &= 0 + 56{,}208.7654 \cdot x - 8.2642 \cdot x^2, \\
M_z &= 0 - 3382.1138 \cdot x + 0.49737 \cdot x^2, \\
M_w &= 0 + 856.7814 \cdot 2{,}179{,}723.9601 \cdot \left(1 - \cosh(\epsilon x) + \tanh\left(\frac{6800\epsilon}{2}\right) \cdot \sinh(\epsilon x)\right), \\
E_1 &= 12, \\
N &= 0
\end{aligned}$$

and have minor fluctuations due to the FE-grid. In the sequel, a cross-validation approach for verification is used. Concretely, the stresses in traces 2–7 were used for estimation and the stress in trace 1 (all internal forces occur in trace 1) for verification, compare Fig. 6 and Eqs. (2)–(8). Thus, the residuals are given by

$$\epsilon_x = \varsigma_1(x) - \left(\frac{z_1}{i_y}\hat{M}_y(x) + \frac{y_1}{i_z}\hat{M}_z(x) + \frac{q_1}{i_w}\hat{M}_w(\varepsilon x) + \hat{E}_1 + \hat{N}\right)$$

for known constants from geometry.

For 69 (0 mm, 100 mm, …, 6800 mm) equidistant values for the stresses the following estimates are obtained:

$$\hat{M}_y = 0 + 56{,}208.5503 \cdot x - 8.2641 \cdot x^2,$$

$$\hat{M}_z = 0 - 3382.1138 \cdot x + 0.49737 \cdot x^2,$$

$$\hat{M}_w = 856.7814 \cdot 2{,}179{,}723.9599 \cdot \left(1 - \cosh(\varepsilon x) + \tanh\left(\frac{6800\varepsilon}{2}\right) \cdot \sinh(\varepsilon x)\right),$$

$$\hat{E}_1 + \hat{N} = 12$$

with residual mean $\mu = 0.012$ and standard deviation $\sigma = 0.16$ which is close to the non-equidistant (69 points randomly chosen) case:

$$\hat{M}_y = 0 + 56{,}207.8515 \cdot x - 8.264 \cdot x^2,$$

$$\hat{M}_z = 0 - 3382.1142 \cdot x + 0.49737 \cdot x^2,$$

$$\hat{M}_w = 856.7814 \cdot 2{,}179{,}923.3682 \cdot \left(1 - \cosh(\epsilon x) + \tanh\left(\frac{6800\epsilon}{2}\right) \cdot \sinh(\epsilon x)\right),$$

$$\hat{E}_1 + \hat{N} = 12$$

with residual mean $\mu = 0.013$ and standard deviation $\sigma = 0.18$.

A Monte-Carlo study with 1,000,000 independent repetitions leads, for 69 equidistant noisy (additive independent zero-mean normally distributed error terms, standard deviation σ) stresses, to the following estimated residual means, standard deviations and repetitions of step 6 (upper limit 100 was never reached):

σ	5	10	25	50	75	100
Residual mean	–0.089	–0.104	–0.054	0.107	0.224	0.0189
Residual standard deviation	0.821	1.158	2.491	4.848	7.269	9.711
Mean number of iterations	2	5	7	11	15	21

which demonstrates principal applicability of the estimation technique.

5.2 A real data example

A bending test has been done in the material testing institute's lab with an S235 steel beam (yield strength 235 MPa, profile IPE300, length 2000 mm) and an evenly distributed load applied in the section 850 mm to 1350 mm. The raw data obtained in the lab test, without any preprocessing, are obviosly error prone, as been shown in the following, non-rescaled, Fig. 16. The load q is choosen to induce a stress up to 235 MPa in the section 850 mm to 1350 mm of the beam. A first step is the elimiation of the outlier in the data using the technique presented in Sect. 4.2.2 and reduction of dependencies according to Sect. 4.2.3. This increases the data's quality dramatically. As there is neither warping torsion nor bending around the second axis, the estimation reduces to one internal force only. A least squares approach on the one hand and a robust least squares approach on the other hand leads to the following results, illustrated in Fig. 17: Here, the maximal structural deviation of the least squares approach is quite large (22.3 MPa) in contrast to the robust least squares (7.5 MPa using Huber-weightening). This underlines the real applicability of the (statistically) robustified technique.

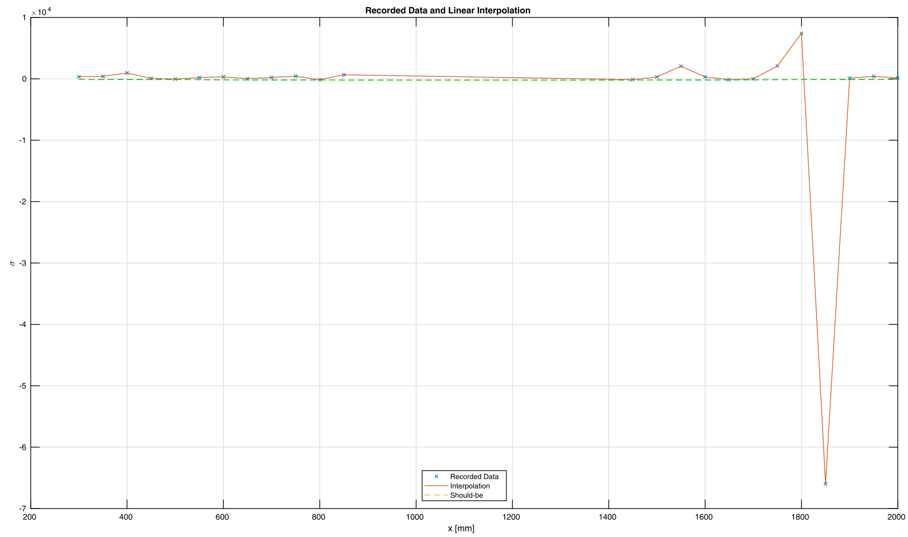

Figure 16 The non-scaled initial data. Several outliers due to dramatically missevaluated AScans are obvious and corrected in a preprocessing step before further estimation

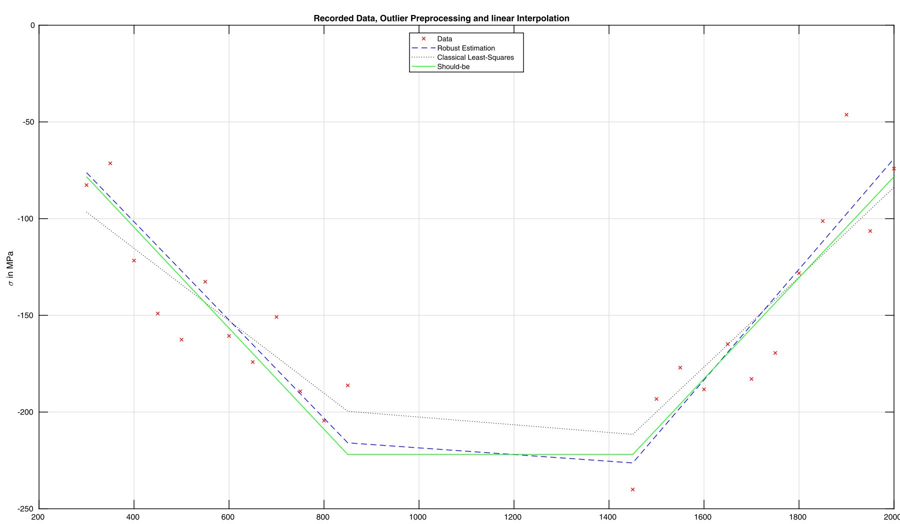

Figure 17 The final estimation of the lab tested, coated beam. The classical approach leads to an unsatisfactory evaluation. Therefore, a robust weight function has been in use too, which improves the results and comes close to the underlying structure

6 Conclusion and further developments

Non-destructive testing is always in competition with destructive testing. Using a combination of micromagnetic and ultrasonic measurements it has been shown that the reserve of resistance of existing steel buildings can be determined non-destructively. The occurring dependencies in the steal beam were modeled and approximated to obtain a weaker dependency structure. For the estimation of internal forces the traces have been chosen to contain all necessary informations but keep the mathematical model handable. The combination of different nonparametric estimation techniques and stepwise robust least square estimation leads to surprisingly good results, even for small sample sizes. Furthermore, these estimation techniques can be further generalised in a future work to a robust setting (e.g. optimally bias robust estimators) to keep applicability for e.g. coated beams. This ends up in new and improved security, usage and sustainability concepts for existing buildings including all relevant internal forces.

Acknowledgements
Special thanks to Claudia Redenbach and Peter Ruckdeschel for several fruitful discussions about mathematics and its implementation. Further, thanks to Claudia Seck and Nicole Schmeckebier for fruitful discussions regarding structural analysis.

Funding
This contribution uses results obtained in the research project *Bestandsbewertung von Stahlbauwerken mithilfe zerstörungsfreier Prüfverfahren* supported by the Forschungsvereinigung Stahlbau in the context of IGF (IGF-Vorhaben 466 ZN) based on a resolution of the German Bundestag as well as the AiF-ZIM-Project *Bestandsbewertung von Stahlbauwerken mithilfe zerstörungsfreier Prüfverfahren*, FZ: ZF4163502LT6, by the Federal Ministry of Economic Affairs and Energy.

Abbreviations
Not applicable.

Availability of data and materials
Please contact author for data requests.

Competing interests
The authors declare that they have no competing interests.

Authors' contributions
The main idea of this paper was proposed by MD and the implementation was also done by MD. JPS supported MD in mathematical modeling as well as in validation. The general engineering context was proposed by WK and CF. CF and WK assisted MD in mechanical modeling and JPS helped preparing the manuscript. All authors read and approved the final manuscript.

Publisher's Note

Springer Nature remains neutral with regard to jurisdictional claims in published maps and institutional affiliations.

Received: 16 February 2018 Accepted: 8 October 2018 Published online: 16 October 2018

References

1. Beuth-Verlag: DIN 1055-100: Einwirkungen Auf Tragwerke - Teil 100: Grundlagen der Tragwerksplanung - Sicherheitskonzept und Bemessungsregeln. Berlin. 2001-03.
2. Normenausschuss Bauwesen (NABau) im DIN Deutsches Institut für Normung e.V.: DIN 1076: Ingenieurbauwerke Im Zuge Von Straßen und Wegen. Überwachung und Prüfung. Berlin. 1999.
3. Deutsche Bahn AG: Richtline DS 805, Tragsicherheit Bestehender Brückenbauwerke. Berlin. 2002.
4. Boller C, Altpeter I, Dobmann G, Rabung M, Schreiber J, Szielasko K, Tschunky R. Electromagnetism as a means for understanding material mechanics phenomena in magnetic materials. Materialwissenschaft und Werkstofftechnik. 2011;42:269–77.
5. Boller C, Starke P. Enhanced assessment of ageing phenomena in steel structures based on material data and non-destructive testing. Mater Sci Eng Technol. 2016;47:876–86.
6. Schneider E, Bindseil P, Boller C, Kurz W. Stand der entwicklung zur zerstörungsfreien bestimmung der längsspannung in bewehrungsstäben in betonbauwerken. Beton und Stahlbetonbau. 2012;107(4):244–54.
7. Fox C, Doktor M, Schneider E, Kurz W. Beitrag zur bewertung von stahlbauwerken mithilfe zerstörungsfreier prüfverfahren. Stahlbau. 2016;85(1):1–15.
8. Mayer JP. Aufbau und Kalibrierung Eines Magnetischen Hall-Sensors zur Detektion und Bewertung Von Schädigung an Stahlbauwerken. Seminar project. Institute of Materials Science and Engineering, University of Kaiserslautern; 2016.
9. Kurz W, Fox C, Doktor M, Hanke R, Kopp M, Schwender T, Nüsse G. Bestandsbewertung Von Stahlbauwerken Mithilfe Zerstörungsfreier Prüfverfahren (P 859). Düsseldorf: Forschungsvereinigung Stahlanwendung e.V. (FOSTA); 2016.
10. Kurz W, Fox C. Evaluation of steel buildings by means of non-destructive testing methods. Schriftenreihe des Studiengangs Bauingenieurwesen der TU Kaiserslautern, Band 18; 2014.
11. Lerman PM. Fitting segmented regression models by grid search. J R Stat Soc, Ser C, Appl Stat. 1980;29(1):77–84.
12. The Mathworks Inc. MATLAB and statistics toolbox release 2017. 2017. Natick: The Mathworks Inc.
13. R Developement Core Team. R: a language and environment for statistical computing. R Foundation for Statistical Computing; 2017.
14. Francke W, Friemann H. Schub und Torsion in Geraden Stäben. Wiesbaden: Vieweg; 2005.
15. Roy SN, Bargmann RE. Tests of multiple independence and the associated confidence bounds. Ann Math Stat. 1958;29(2):491–503.
16. van der Vaart AW. Asymptotic statistics. Cambridge: Cambridge University Press; 2012.

17. Hampel FR, Ronchetti EM, Roussew PJ, Stahel WA. Robust statistics, the approach based on influence functions. Wiley series in probability and statistics. Indianapolis; 2005.
18. Ackermann J. Die barkhausen-rauschanalyse zur ermittlung von eigenspannungen im stahlbau [PhD thesis]. Darmstadt University, Department of Civil Engineering; 2008.
19. Brockwell PJ, Davis RA. Introduction to time series and forecasting. New York: Springer; 2002.
20. Holland PW, Welsch RE. Robust regression using iteratively reweighted least-squares. Commun Stat, Theory Methods. 1977;6(9):813–25.
21. Levenberg K. A method for the solution of certain non-linear problems in least squares. Q Appl Math. 1944;2(2):164–8.
22. Marquardt DW. An algorithm for least-squares estimation of nonlinear parameters. J Soc Ind Appl Math. 1963;11(2):431–41.
23. Györfi L, Kohler M, Krzyzak A, Walk A. A distribution-free theory of nonparametric regression. New York: Springer; 2010.
24. Thein C. Sicherheitskonzept Eines Zerstörungsfrei Geführten Tragfähigkeitsnachweises [BSc thesis]. Department of Civil Engeneering, University of Kaiserslautern; 2017.